Journal of University of Science and Technology Beijing
Volume 11, Number 6, December 2004, Page 489

Experimental study of a technique for load measurement of powered supports

Hua Zhu, Shirong Ge, Xiaolong Huang, and Sumei Dai

College of Mechatronic Engineering and Material Science, China University of Mining and Technology, Xuzhou 221008, China

(Received 2003-12-29)

Abstract: Despite the increasing popularity of mechanized coal mining, there are no convenient and accurate means available to measure the loads of powered supports. The measurement of such loads is important for monitoring mine pressure and ensuring production safety. The load-carrying features of a powered support were used to develop a method for load measurement using the magnetoelastic principle. A cross bridge-type magnetoelastic stress sensor was designed for the support structures to measure the different parts of the supports. Tests on single-body hydraulic cylinders and simulated linkages showed that an approximately linear relationship between the values of the sensor output signal and the loads borne by the hydraulic cylinders or linkages. The results were used to analyze the load-carrying measurements of powered supports with the cross bridge-type magnetoelastic stress sensor.

Key words: powered support; load measurement; stress; magnetoelastic; sensor

[*The work was financially supported by the National Natural Science Foundation of China (No. 50225519) and the Natural Science Foundation of Jiangsu Province (No. BK2002116).*]

1 Introduction

In large coal mines, the hydraulic support is one of the chief coal mining equipment. It is used for rock pressure support at the fully mechanized coalfaces. Despite its increasing popularity in coal mining there is no convenient and accurate means available to measure its supporting load. As the hydraulic support has complex structures, load measurement is very difficult, which has become a major problem in the application of hydraulic supports [1-4]. A quick, convenient and precise intelligent instrument is needed for load measurement of hydraulic supports. A key technique is to measure the stress in some parts of the hydraulic support. A cross bridge-type magnetoelastic stress sensor (CBMSS) was developed based on ferromagnetic theories and the structural features of the powered supports to provide load measurement of hydraulic supports. This paper explains the CBMSS structure, and the principle and method for the mechanical stress measurement. The load measuring results are presented using simulated linkages and single-body hydraulic cylinders.

2 Structure of CBMSS and the principle of stress measurement

According to ferromagnetic theory [5], ferromagnetic materials have magnetoelastic or magnetoimpedance behavior induced by the variation of the magnetic intensity of the materials, due to the mechanical stress when external forces act upon them. The inverse to the magnetoelastic effect is the magnetostrictive effect. The mechanical stress or distortion of ferromagnetic materials changes the intensity of the magnetic field in ferromagnetic materials.

Different types of magnetoelastic stress sensors (MSS) can be designed to measure the mechanical stress in ferromagnetic materials based on the above principles [6]. The CBMSS was developed according to the hydraulic support structures which fit to measure the stresses at different parts of the supports. The basic structure of the CBMSS is shown in **figure 1**. It consists of two U-shaped excitation and detection cores sintered from ferrite powders crossing orthogonally in space. A pair of excitation and detection coils are wound around the bases of the two cores. When measuring loads, the cores are placed perpendicular to a specimen at specified intervals, so a magnetic bridge circuit is formed from four magnetic resistances (R_1, R_2, R_3 and R_4) of the material between two adjacent magnetic poles among the four poles (D_1, D_2, D_3 and D_4) as shown in **figure 2**.

Corresponding author: Hua Zhu, **E-mail:** hzhu@cumt.edu.cn

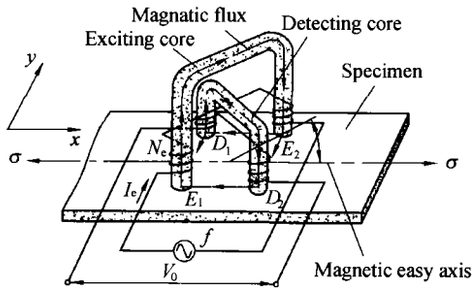

Figure 1 Basic CBMSS structure.

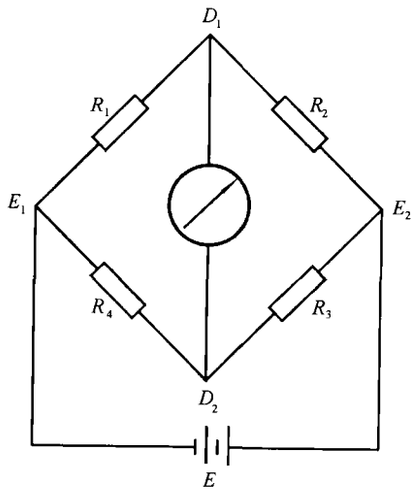

Figure 2 CBMSS bridge circuit.

When a current with a specified frequency is applied to the excitation coils, an alternating flux is formed in its core to excite the specimen. Before a force acts on the specimen no internal stresses exist in the material and the magnetism of the material surface is isotropic; therefore, the magnetic conductivity (or magnetic resistance) of each of the bridge arms is the same. The magnetic bridge is balanced, with no induced electromotive force in the detection coils, so no voltage signals are output from the CBMSS. Internal stresses appear in the specimen when a force is applied. For the force illustrated in figure 1, the tensile stress is induced in the direction of x axis with the pressure stress along y axis. As a result, the opposite changes occur in the magnetic conductivity in the two directions, that is, the magnetic conductivity in x direction increases and that in y direction decreases. Therefore, the balance of the magnetic bridge will be upset, and the electromotive force will be induced from the detection coils. Consequently, voltage signals are the output from the CBMSS.

The CBMSS output voltage V_0 can be represented by the following expression [7]:

$$V_0 = V_m \left\{ \frac{\mu_x}{\sqrt{1-\xi^2\cos^2(\theta-45^\circ)}} - \frac{\mu_y}{\sqrt{1-\xi^2\sin^2(\theta-45^\circ)}} \right\} \quad (1)$$

where $V_m = \omega N_e N_d I_e K_m \mu_0 / 2m$, V. ω: the excitation angular frequency, $\omega = 2\pi f$; N_e: the number of excitation coil windings; N_d: the number of detecting coil windings; I_e: the excitation current, A; K_m: the amplification factor; μ_0: the magnetic conductivity of cores; $m = l/A$; l: the magnetizing path length, m; A: the cross sectional area, m^2; $\xi = \sqrt{1-\alpha^2}$, $\alpha = \mu_y / \mu_x$; μ_x: the magnetic conductivity in x direction, μ_y: the magnetic conductivity in y direction; θ: the angle of the magnetization-easy axis of the specimen and the pair of excitation cores.

The tensile stress in x direction extends the specimen in x direction and contracts it in y direction. If θ is not zero, a voltage signal is generated in the detection coils. As long as the magnetic conductivity of the specimen changes linearly with stress, the output voltage from the sensor also shows a linear relationship to stress.

3 Load-measuring approach of powered supports

Figure 3 shows a schematic diagram of a chock-shield type powered support and its load distribution. The support is composed of a top beam, shield beam, hydraulic posts, linkages, balance lifting jacks and base. The external load directly acts on the top beam and the shield beam, and it is transferred through the hydraulic posts and linkages to the base. According to static theory, as long as the force on the hydraulic posts and linkages can be measured, the total external load imposed upon the powered support can be calculated as a function of the geometric and operating parameters of the powered support [8].

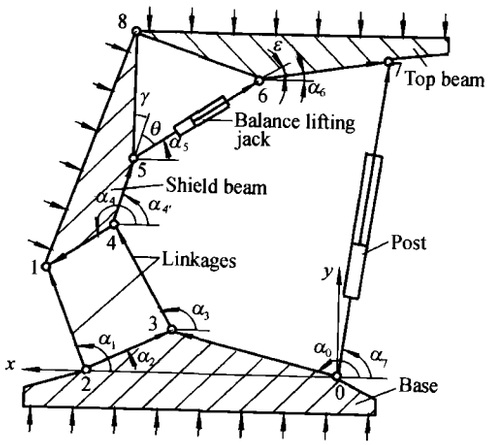

Figure 3 Schematic diagram of a powered support and its load distribution.

Because of the liquid pressure, the tensile stress is

formed in the circumferential direction of the cylinder of the hydraulic post, and the stress in the axial direction of the cylinder is almost zero. The linkage is commonly a planar or columnar structure. The linkage can be analyzed as a one-dimensionally forced pole, which only bears tensile or compressive stresses. The mechanical stress on the hydraulic cylinder and linkages shows the magnitude of the load acting upon the powered support.

According to equation (1), if θ is equal to 45°, then

$$V_0 = V_m \frac{\mu_x^2 - \mu_y^2}{\mu_y} \tag{2}$$

Equation (2) shows that the output voltage is at maximum for a given load when the angle between the pair of excitation cores and the magnetic easy axis of the specimen is 45°. Therefore, the best effect of load measurement is obtained at this measuring angle. Hence, for the CBMSS with the stress characteristics of the hydraulic posts and linkages, as long as any two adjacent core feet of the CBMSS are parallel or perpendicular to the post or linkage axe, the best measuring condition can be satisfied. Diagrams of these load-measuring positions are shown in **figures 4** and **5**.

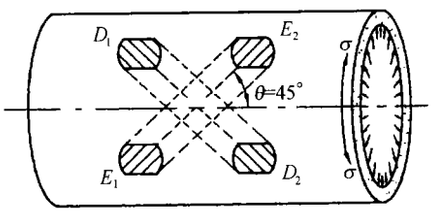

Figure 4 Diagram of load measurement points.

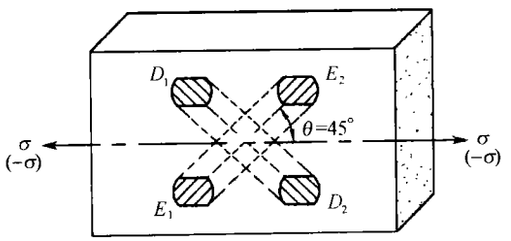

Figure 5 Diagram of load measurement points on a linkage with CBMSS.

4 Experimental

4.1 Procedure

Three load measuring tests were carried out with the CBMSS.

Test one: tensile stress measurement. The testing specimen was carbon steel with a hardness of HRC23 and its dimensions are shown in **figure 6**. The load tests were conducted on a fatigue tester with the magnitudes of the applied loads from 0 to 182 MPa.

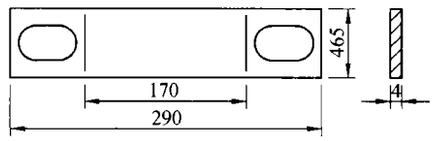

Figure 6 Tensile stress measurement specimen dimensions (unit: mm).

Test two: compressive stress measurement. The testing specimen was also carbon steel with a hardness of HRC22 and a dimension of 87 mm×45 mm×22 mm. The load tests were also conducted on the fatigue tester with the magnitudes of the applied loads from 0 to 150 MPa.

Test three: liquid pressure measurement. The testing specimen was a single-body hydraulic cylinder with standard size: DZ12-25/80. The cylinder was made of a seamless steel tube with an inner diameter of 80 mm and a thickness of 12 mm. The load tests were conducted on a vertical hydraulic tester with the magnitudes of the applied liquid pressure from 0 to 45 MPa. The block diagram of the load measurement system is shown in **figure 7**.

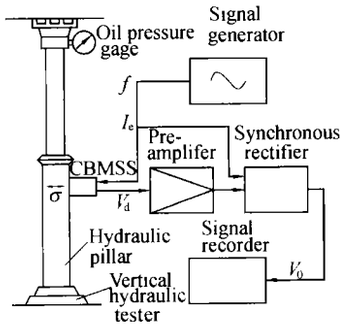

Figure 7 Block diagram of the measurement system for the hydraulic cylinder with CBMSS.

4.2 Test results

Different loads were applied to the specimens within their elastic ranges, and the output voltages were measured with a calibrated CBMSS. The current with definite frequency was applied to the excitation coils to produce the loads and output voltages, as shown in **tables 1-3** and **figures 8-10**.

4.3 Analysis of the test results

The experimental results show that:

(a) The sensor output voltages varied tremendously with the applied loads.

(b) Because the material has different permeabilities for tensile and compressive stresses, the slopes of the voltage-stress curve of the tensile test were different from that of the compressive test.

Table 1 Tensile stress measurement results

Order	Load / MPa	Voltage / mV	Error / mV	Unloading / mV	Error / mV
1	0	0	0	47.6	–0.3-0.2
2	13	10.1	–0.1-0.1	50.0	–0.2-0.1
3	26	15.8	–0.1-0.0	59.4	–0.2-0.2
4	39	19.0	–0.1-0.2	66.8	–0.3-0.2
5	52	23.3	–0.1-0.2	78.0	–0.1-0.2
6	65	30.5	–0.2-0.1	87.9	–0.2-0.3
7	78	38.6	–0.1-0.2	96.3	–0.3-0.2
8	91	46.8	–0.2-0.2	112.0	–0.1-0.3
9	104	61.3	–0.1-0.2	124.5	–0.3-0.2
10	117	77.0	–0.1-0.1	132.0	–0.2-0.3
11	130	94.1	–0.2-0.2	144.0	–0.1-0.3
12	143	106.7	–0.2-0.3	153.6	–0.1-0.4
13	156	126.0	–0.1-0.2	157.0	–0.2-0.3
14	169	144.5	–0.3-0.2	163.8	–0.2-0.2
15	182	168.4	–0.4-0.2	168.4	–0.4-0.2

Table 2 Compressive stress measurement results

Order	Load / MPa	Voltage / mV	Error / mV	Unloading /mV	Error / mV
1	0	0	0	–19.9	–0.3-0.2
2	–10	–3.2	–0.1-0.0	–22.0	–0.1-0.2
3	–20	–6.6	–0.1-0.0	–28.8	–0.2-0.2
4	–30	–8.0	–0.0-0.1	–31.9	–0.1-0.3
5	–40	–12.7	–0.1-0.1	–33.5	–0.1-0.2
6	–50	–14.8	–0.1-0.2	–35.4	–0.1-0.3
7	–60	–17.0	–0.2-0.1	–40.0	–0.2-0.2
8	–70	–19.1	–0.1-0.2	–41.7	–0.2-0.2
9	–80	–22.5	–0.1-0.3	–43.2	–0.1-0.4
10	–90	–28.6	–0.2-0.2	–44.9	–0.1-0.3
11	–100	–32.0	–0.1-0.2	–48.0	–0.3-0.1
12	–110	–36.9	–0.2-0.2	–49.8	–0.4-0.2
13	–120	–41.5	–0.3-0.1	–51.3	–0.2-0.2
14	–130	–46.5	–0.2-0.3	–52.8	–0.2-0.3
15	–140	–49.8	–0.3-0.2	–52.9	–0.2-0.2
16	–150	–53.0	–0.4-0.2	–53.0	–0.4-0.2

Table 3 Hydraulic cylinder load test results

Order	Load / MPa	Voltage / mV	Error / mV	Unloading / mV	Error / mV
1	0	0	0	14.0	–0.1-0.3
2	5	2.5	–0.1-0.1	18.0	–0.3-0.2
3	10	7.0	–0.1-0.2	23.0	–0.3-0.2
4	15	9.5	–0.1-0.1	28.5	–0.1-0.3
5	20	14.0	–0.1-0.2	32.0	–0.1-0.2
6	25	18.0	–0.2-0.2	35.5	–0.2-0.2
7	30	25.5	–0.1-0.1	40.0	–0.1-0.2
8	35	33.5	–0.2-0.1	42.5	–0.1-0.1
9	40	40.0	–0.2-0.2	45.0	–0.1-0.2
10	45	46.0	–0.3-0.2	46.0	–0.3-0.2

(c) Positive voltages corresponded to tensile stresses, while negative voltages corresponded to compressive stresses, which can identify whether a mechanical component is in tension or compression.

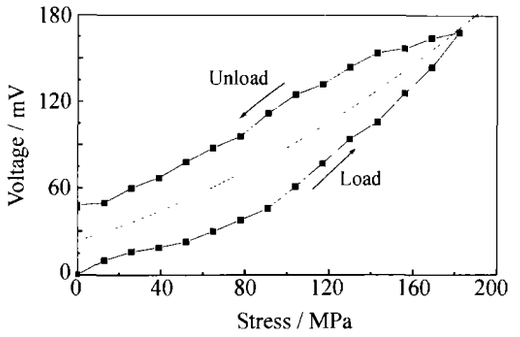

Figure 8 Output voltage-stress curves for tensile stress tests.

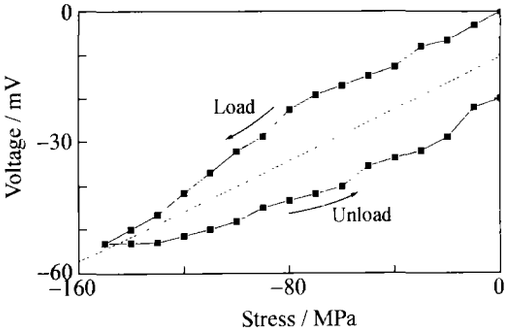

Figure 9 Output voltage-stress curves for compressive stress tests.

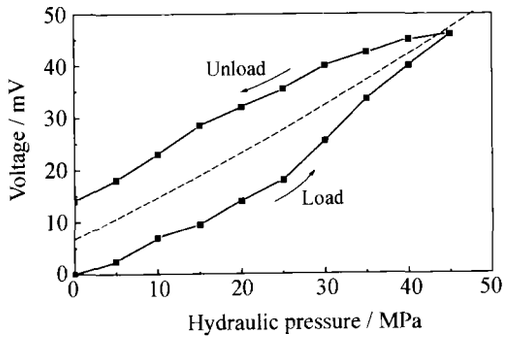

Figure 10 Output voltage-stress curves for cylinder stress tests.

(d) Hysteresis was observed when the specimens were loaded and unloaded. However, because the stresses in the powered support structures change slowly and need not be measured continually at a measuring point for many times, the hysteresis and its influence on the measurements are not serious.

5 Conclusions

The load-carrying features of a powered support were used to design a cross bridge-type magnetoelastic stress sensor to measure the stresses in different parts of the powered support. The application of the sensor to single-body hydraulic cylinders and simulated linkages show that there is an approximately linear relationship between the sensor output signal and the load born by the hydraulic cylinders or linkages. Therefore, the sensor can be used to measure the loads on hydraulic posts and linkages of powered supports. The total external load imposed upon the powered support can then be calculated as a function of its geometry and operating parameters, including the magnitude, direction and location of the load. Therefore, the sensor can be used to develop a portable intelligent load-measuring instrument, with signal processing techniques and load calculation software, to measure and display the loads of powered supports in-situ.

References

[1] S.K. Das, Determination of optimum capacity of powered roof supports in the longwall face in medium thick coal seam [J], *J. Mines Met. Fuels*, 43(1995), No.5, p.99.

[2] R. Singh and T.N. Singh, Investigation into the behaviour of a support system and roof strata during sublevel caving of a thick coal seam [J], *Geotech. Geol. Eng.*, 17(1999), No.1, p.21.

[3] V.I. Klishin and Y.V. Matviets, Increase of single-row powered roof support adaptation to conditions of loading [J], *Fiziko-Tekhnicheskie Problemy Razrabotki Poleznykh Iskopaemykh* (in Russian), 1993, No.2, p.23.

[4] Y.W. Shi, Behavior of rocks and mechanical model of loads on the powered supports in a fully mechanized sublevel caving face [J], *J. China Coal Soc.* (in Chinese), 22(1997), No.6, p.253.

[5] W.D. Zhong, *Ferromagnetism* (in Chinese) [M]. Science Press, Beijing, 1987.

[6] F.Z. Wu, *Torque Sensors of Magnetic Anisotropy* (in Chinese) [M]. Measure Publishing Company, Beijing, 1985.

[7] H. Wakiwaka, Stress measurement using a magnetic anisotropy sensor utilizing AC demagnetization [J], *Magn. Soc. Jpn.*, 14(1990), No.2, p.387.

[8] H. Zhu, X.Y. Yu, S.R. Ge, and S.B. Wang, Methods for measuring and calculating the external load of powered supports [J], *J. Univ. Sci. Technol. Beijing*, 10(2003), No.6, p.11.